International Journal of Minerals, Metallurgy and Materials
Volume 21, Number 4, April 2014, Page 371
DOI: 10.1007/s12613-014-0918-5

In situ measured growth rates of bainite plates in an Fe–C–Mn–Si superbainitic steel

Zhang-wei Hu[1)], *Guang Xu*[1)], *Hai-jiang Hu*[1)], *Li Wang*[2)], *and Zheng-liang Xue*[1)]

1) Key Laboratory for Ferrous Metallurgy and Resources Utilization of the Ministry of Education, Wuhan University of Science and Technology, Wuhan 430081, China
2) State Key Laboratory of Development and Application Technology of Automotive Steels (Baosteel Group), Shanghai 201900, China
(Received: 12 September 2013; revised: 5 December 2013; accepted: 9 December 2013)

Abstract: The growth rates of bainite plates in an Fe–C–Mn–Si superbainitic steel were investigated by *in situ* observation. The lengthening rates of ferrite bainite during both cooling and isothermal holding processes were observed and the growth rates of bainite plates nucleating at grain boundaries, within grains and on preformed bainite were measured. It is indicated that the lengthening rates of bainite plates during the cooling and isothermal processes were different, and that the growth rates of bainite plates nucleating at different types of sites also demonstrated diversity. The bainite plates initiating at grain boundaries during cooling grew the fastest, while the plates nucleating on preformed bainite did the slowest. However, the growth rate of the bainite plates nucleating at grain boundaries during isothermal transformation decreased the most, whereas the bainite plates initiating within grains grew the fastest. In addition, the growth rate of ferrite bainite in the study supported the diffusion transformation mechanism of bainite from the viewpoint of growth rate.

Keywords: bainitic steel; bainite; growth rate; cooling; isothermal treatment; phase transitions

1. Introduction

Bainitic steels possessing both high strength and good toughness have always been a topic of interest in steel research [1–2]. The kinetics of bainitic transformation has been studied quite extensively for a few decades, with the growth rate of bainite plates being one of the main research interests in phase transformation kinetics. Some recent work has been conducted on the growth rate of ferrite bainite. Yada and Ooka [3] calculated the growth rates of typical upper and lower bainite plates by hot-stage *in situ* optical microscopy. Yada *et al.* [4] also investigated the lengthening of bainite plates in an Fe–0.7C–6Ni alloy during transformation by hot-stage electron microscopy. Moreover, Matas and Hehemann [5], and Nemoto [6] reported experimental data for the growth rate of bainitic laths in Fe–0.5C–Ni alloys. Quidort and Brechet [7] calculated the growth rate of bainite in 0.5% C steels with the Trivedi equation and claimed that the model for carbon diffusion could satisfactorily predict the temperature and carbon content dependencies of growth rate. In addition, some experimental investigations by *in situ* observation or hot-stage optical microscopy indicated that the lengthening of bainite laths proceeds at a constant rate [8–10]. Further, Speich and Cohen [11], employing a hot-stage microscope to study the growth kinetics of bainite plates, reported that the lengthening rate is well consistent with values calculated by the models of carbon diffusion control [12–13].

Almost all of the recent studies focused on bainite plate lengthening during isothermal holding. However, these studies did not distinguish between the lengthening discrepancies that might arise from bainite nucleation at different sites. In the present study, the growth processes of bainite plates in a superbainitic steel were dynamically observed by laser scanning confocal microscopy (LSCM). The growth rates of bainite plates during both cooling and isothermal holding processes were investigated, and the lengthening rates of bainite plates nucleating at grain boundaries, within grains and on preformed bainite were measured.

Corresponding author: Guang Xu E-mail: xuguang@wust.edu.cn

2. Experimental

The experimental material is an Fe–C–Mn–Si super-bainitic steel refined in a 25 kg vacuum induction furnace and cast into a small ingot, followed by rolling to a 10-mm-thick flat. The material composition of the steel is listed in Table 1. High-temperature LSCM was chosen as a method for revealing bainite plates for its obvious advantage of *in situ* observation of bainite growth over time. LSCM samples were machined into cylinders of 6 mm in diameter and 4 mm in length. The top and bottom surfaces of the samples were polished to ensure a level measurement face and to minimize the effect of surface roughness. The investigations were performed in a VL2000DX LSCM according to test procedures shown in Fig. 1. The specimen chamber was evacuated to 6×10^{-3} Pa before heating, and argon was used to protect the specimens from surface oxidation. The specimens were heated at a rate of 5°C/s to 1100°C and held for 30 min. Then they were cooled at 5°C/s to 330°C and isothermally treated for 60 min, to allow bainitic transformation, followed by final air cooling to room temperature. The scanning frequency of 15 Hz was chosen for the whole procedure from heating to cooling. A video showing the dynamic growth process of ferrite bainite was simultaneously obtained. The principle for *in situ* observation of bainite nucleation and growth is a relief phenomenon occurring in phase transitions. Ko and Cottrell [14] first observed the relief phenomenon of bainitic transformation in 1952.

Table 1. Material composition of the tested steel wt%

C	Si	Mn	P	S	Al	Ti	N
0.4	2	2.81	0.008	0.003	0.4	0.0017	0.0042

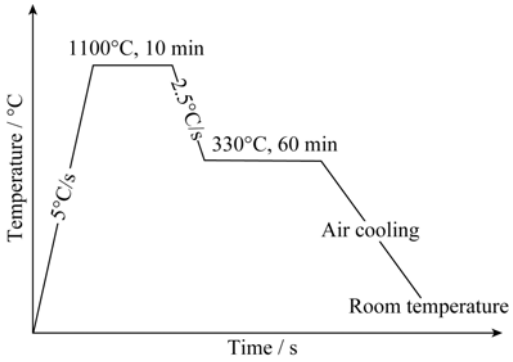

Fig. 1. Heat treatment procedure.

3. Results

3.1. Nucleation and growth of bainite plates

Many studies on nucleation and growth of bainite plates were conducted by conventional metallography. In this study, the dynamic processes of nucleation and growth of bainite plate were directly observed by high-temperature LSCM. Fig. 2 shows micrographs of bainite nucleation taken by LSCM, from which it can be observed that bainite nuclei initiate at three types of sites. Bainite platelets can nucleate at austenite grain boundaries (indicated by arrow a in Fig. 2) or within austenite grains (indicated by arrow b in Fig. 2). Moreover, sympathetic nucleation of bainite platelets is also observed. As indicated by arrow c in Fig. 2, bainite platelets initiate in the same direction as previously formed bainite plates.

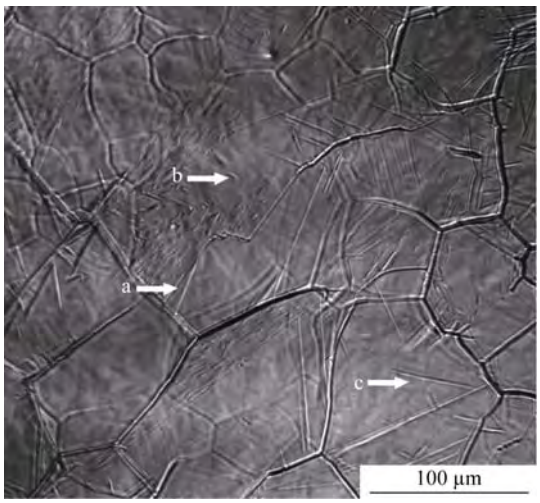

Fig. 2. Nucleation of bainite plates.

3.2. Lengthening of bainite plates during cooling

The process of bainite plate lengthening during cooling was directly observed by *in situ* investigation on the LSCM. The lengthening rate was determined by the slope of the length-to-time plot. Fig. 3 illustrates the lengths of a bainite plate that nucleated at a grain boundary; Fig. 3(a) shows its length at 2164.83 s, and Figs. 3(b) and 3(c) indicate its lengthening over time. The lengthening curve of the bainite plate that nucleated at the grain boundary is plotted in Fig. 3(d) to correspond with the lengths of the bainite plate at different times (Figs. 3(a)–3(c)), and a growth rate of 7.8 μm/s is obtained by the slope of the length-to-time plot.

The growth rates of bainite plates that nucleated within grains or on previously formed bainite plates were obtained in the same way. Fig. 4 shows the LSCM micrographs of a bainite plate that nucleated within a grain at a growth rate of 4.5 μm/s, while Fig. 5 shows the lengthening process of a bainite plate that nucleated on preformed bainite at a growth rate of 1.3 μm/s. By measuring the growth rates of bainite plates that nucleated at different types of sites, it was

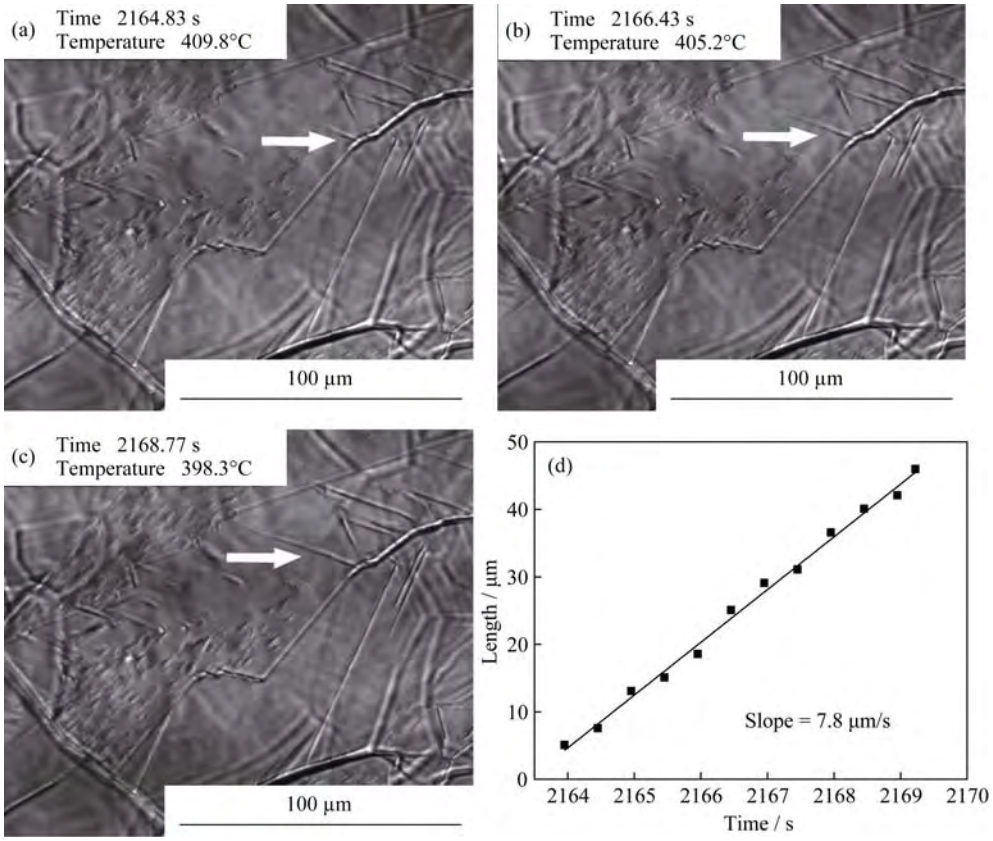

Fig. 3. Micrographs of the growth of a bainite plate that nucleated on a grain boundary during cooling (a–c) and length-to-time plot (d).

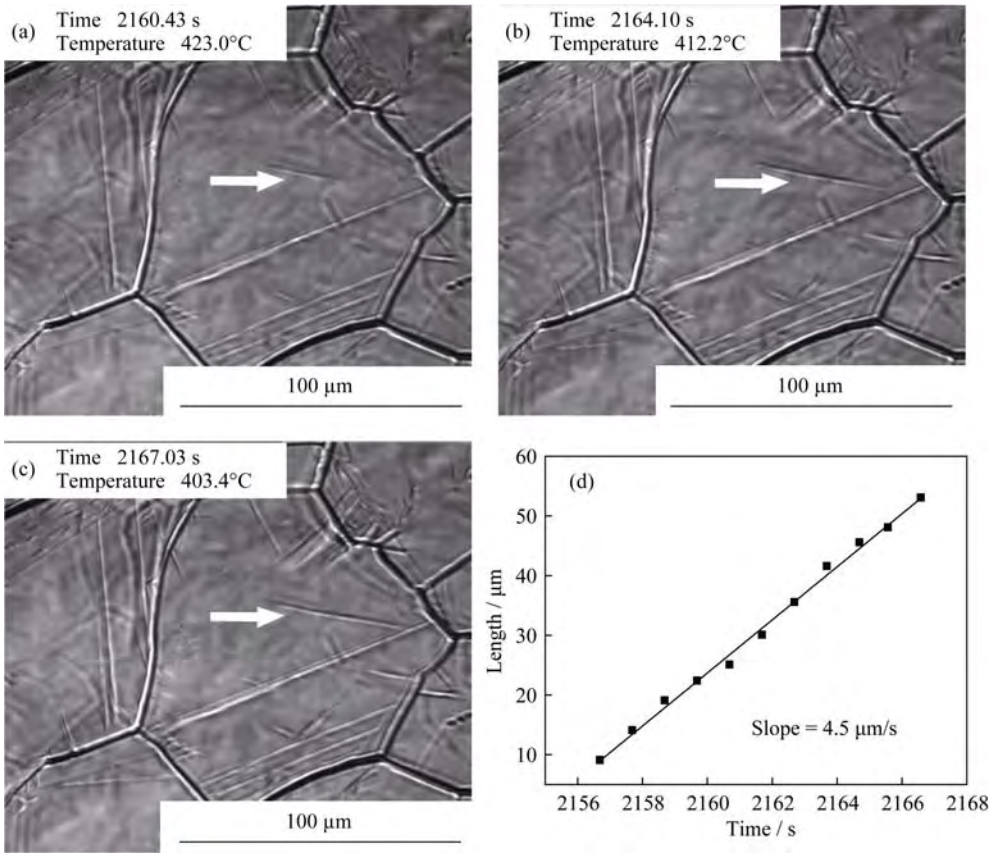

Fig. 4. Micrographs of the growth of a bainite plate that nucleated within a grain during cooling (a–c) and length-to-time plot (d).

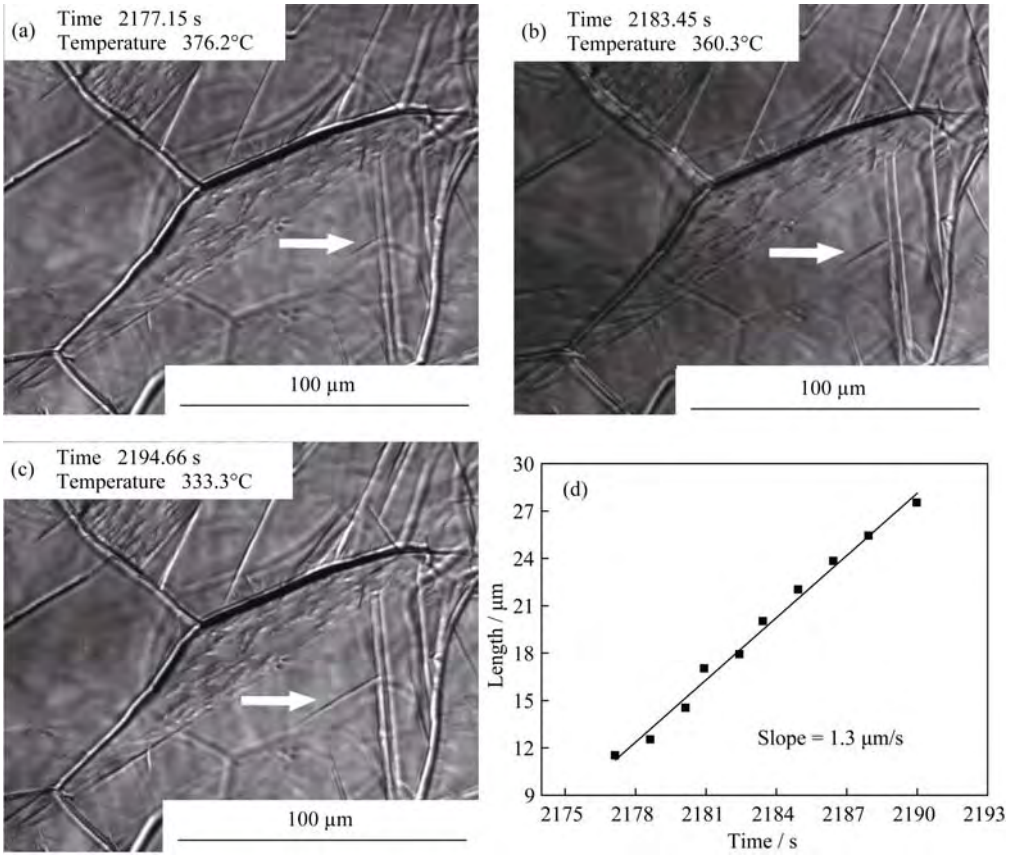

Fig. 5. Micrographs of the growth of a bainite plate that nucleated on a preformed bainite plate during cooling (a–c) and length-to-time plot (d).

observed that the bainite plate initiating at the grain boundary had the fastest growth, whereas the bainite plate nucleating on preformed bainite had the slowest growth. The lengthening rate is constant during the growth process.

3.3. Lengthening of bainite plates during isothermal holding

The growth rates of bainite plates that nucleated at different sites during isothermal holding were determined by the method mentioned above. The lengthening of a bainite plate that nucleated at a grain boundary during isothermal transformation is illustrated in Fig. 6; Fig. 6(a) shows its length at 2195.96 s, and Figs. 6(b) and 6(c) indicate its lengthening over time. The lengthening curve of the bainite plate that nucleated at the grain boundary is plotted in Fig. 6(d) to correspond with the lengths of the bainite plate at different times (Figs. 6(a)–6(c)), and a growth rate of 0.53 μm/s is obtained by the slope of the length-to-time plot.

In addition, the lengthening and growth rates of bainite plates that nucleated within grains and on previously formed bainite are given in Figs. 7 and 8, respectively. The growth rates of bainite plates nucleated within grains and on preformed bainite are 0.86 and 0.84 μm/s, respectively. This indicates that the maximum growth rate was achieved by a bainite plate initiating within a grain, whereas the minimum growth rate was for the one nucleating at a grain boundary. Generally speaking, the growth rate of bainite plates during isothermal holding is lower than that during the cooling process.

4. Discussion

Of the reported work on bainite growth rate, only the average growth rate during the isothermal process has been given, not the differences in the growth rates of bainite plates having different nucleation sites. In the present study, the growth rates of bainite plates that nucleated at different sites during both cooling and isothermal holding processes were calculated based on the lengths of bainite plates at different times observed by LSCM micrographs. Table 2 and Fig. 9 summarize the average growth rates measured during cooling for 18, 16, and 13 bainite plates that initiated at grain boundaries, within grains, and on preformed bainite plates, respectively. Table 3 and Fig. 10 summarize the average growth rates measured during isothermal holding for 16, 12, and 8 plates that initiated as above, respectively.

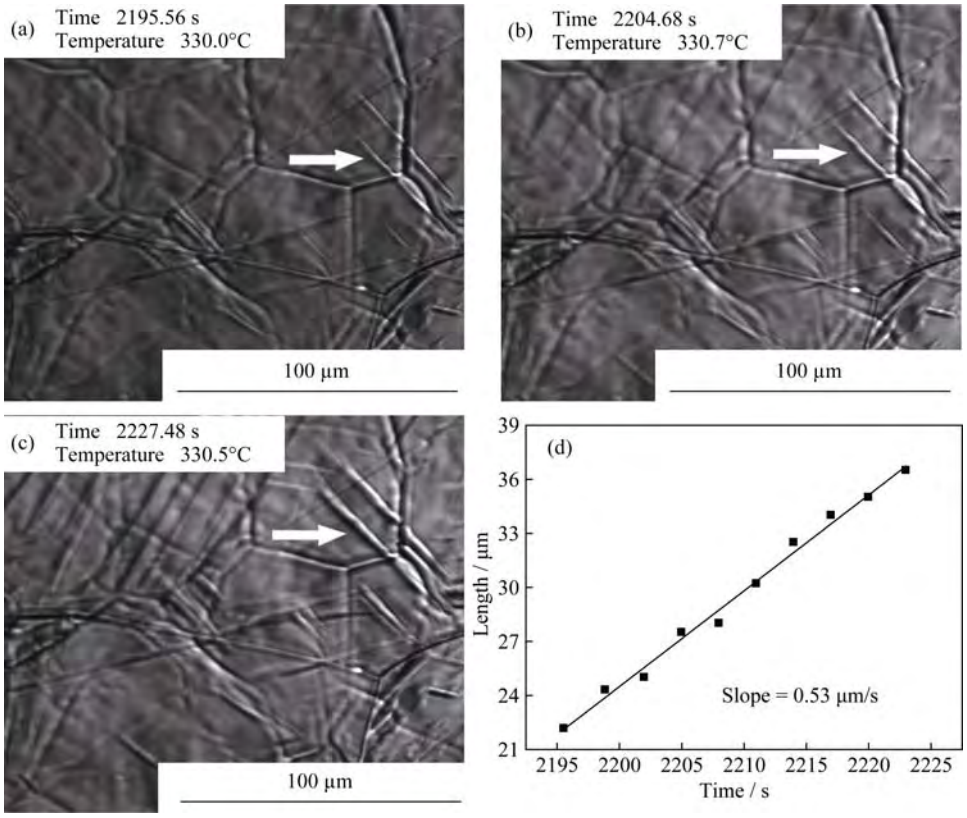

Fig. 6. Micrographs of the growth of a bainite plate that nucleated at a grain boundary during isothermal holding at 330°C (a–c) and length-to-time plot (d).

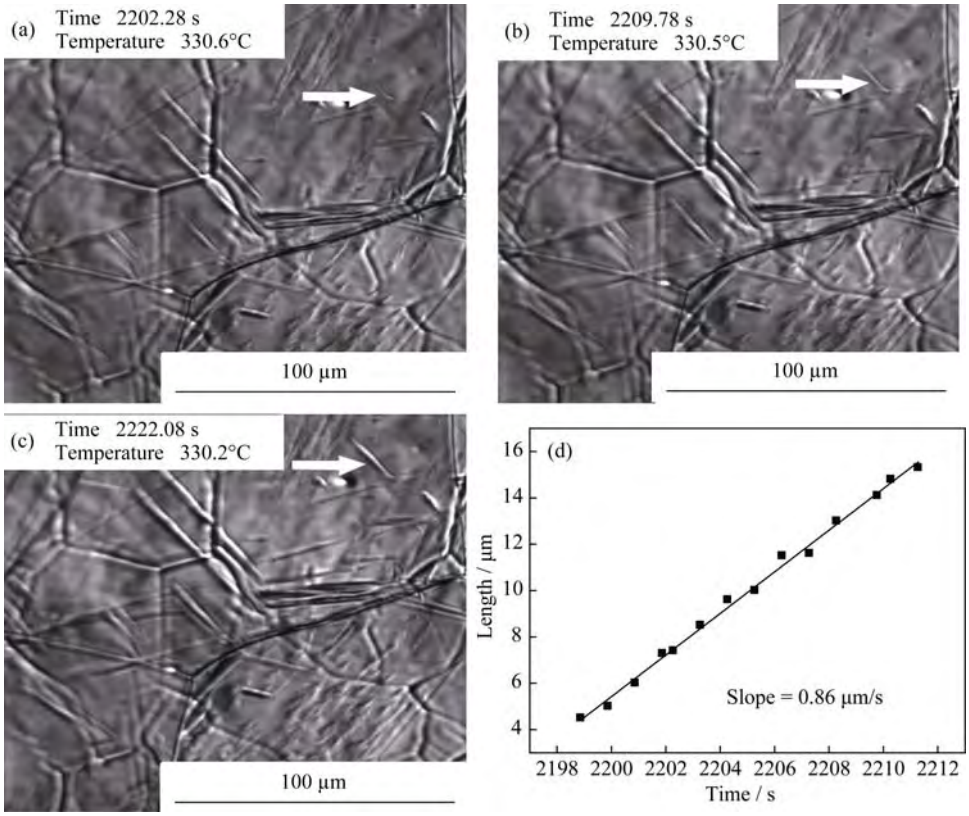

Fig. 7. Micrographs of the growth of a bainite plate that nucleated within a grain during isothermal holding at 330°C (a–c) and length-to-time plot (d).

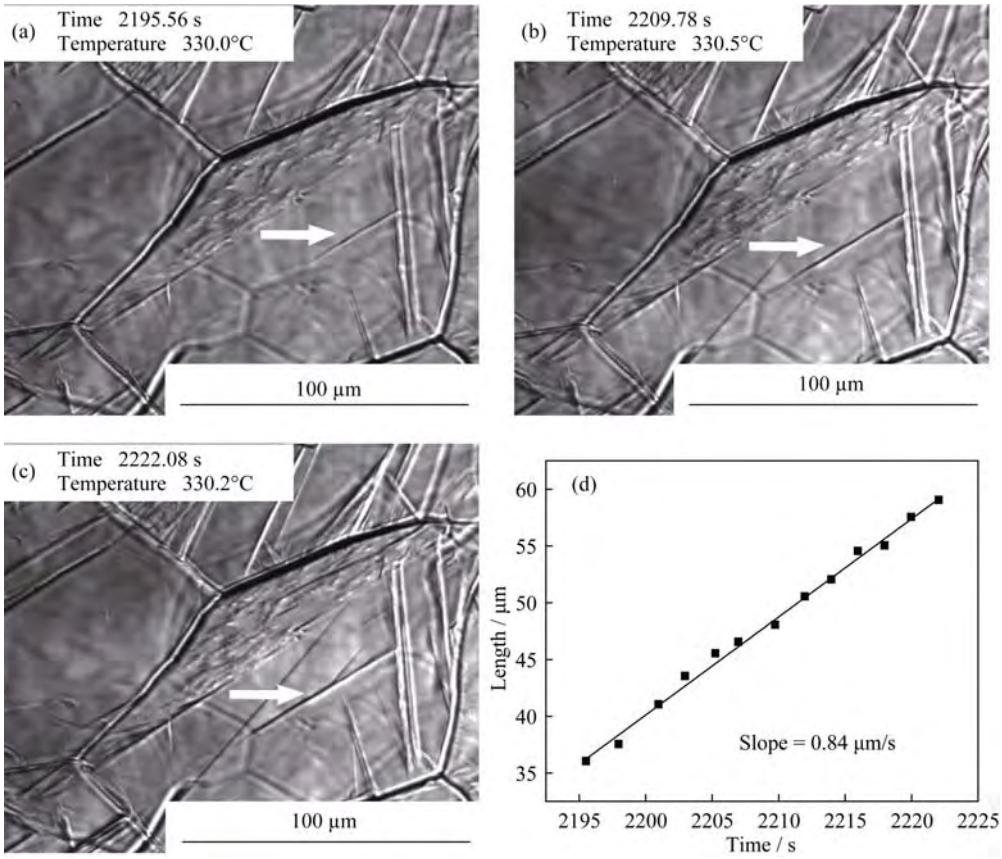

Fig. 8. Micrographs of the growth of a bainite plate that nucleated on a preformed bainite plate during isothermal holding at 330°C (a–c) and length-to-time plot (d).

Table 2. Lengthening rates of bainite plates measured by *in situ* observation during cooling

Nucleation site	Number of plates	Lengthening rate / (μm·s^{-1})			
		Maximum	Minimum	Mean	Standard deviation
At grain boundaries	18	8.2	1.6	5.12	1.93
Within grains	16	5.3	1.1	3.09	1.34
On preformed bainite	13	1.5	0.9	1.21	0.16

It can be observed that the growth rate of bainite plates nucleating at grain boundaries during cooling is the highest, whereas the growth rate of bainite plates nucleating on preformed bainite is the lowest. First, bainite nuclei easily initiate at grain boundaries because of high energy which results from irregular atomic arrangements and lattice distortions. Moreover, the diffusion speed of atoms at grain boundaries is higher owing to the presence of more defects such as dislocations and vacancies. The nucleation and growth of new nuclei at grain boundaries can reduce the grain energy in a spontaneous process. Therefore, the highest average lengthening rate is for bainite plates initiating at grain boundaries.

During isothermal transformation, the lowest average growth rate occurs for bainite plates initiating at grain boundaries. This occurs because the growth rate of bainite plates nucleating at grain boundaries is the highest during the cooling process, at which the growth almost reaches completion. Further, the average lengthening rates of different bainite plates are lower during isothermal holding than those during the cooling process.

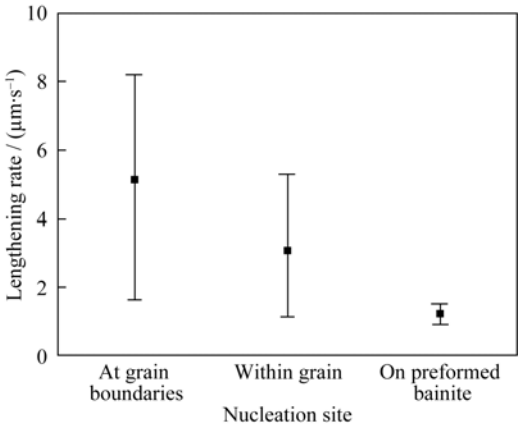

Fig. 9. Average lengthening rates of bainite plates that nucleated at grain boundaries, within grains, and on preformed bainite plates during cooling.

Table 3. Lengthening rates of bainite plates measured by *in situ* observation during isothermal holding

Nucleation site	Number of plates	Lengthening rate / (μm·s^{-1})			
		Maximum	Minimum	Mean	Standard deviation
At grain boundaries	16	0.6	0.1	0.35	0.16
Within grains	12	1.0	0.2	0.62	0.26
On preformed bainite	8	0.9	0.2	0.54	0.25

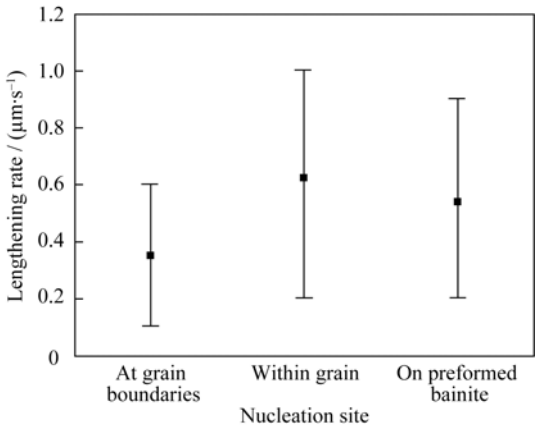

Fig. 10. Average lengthening rates of bainite plates nucleated on grain boundaries, within grains, and on preformed bainite plates during isothermal holding at 330°C.

Diffusion-controlled models for the growth rate of ferrite bainite include the Zener–Hillert equation and the Trivedi equation. The Zener–Hillert [15] equation is as follows:

$$\upsilon_{\max}\rho_c / D = 10^{-2.5(1-\Omega_0)}\Omega_0 / 4(1-\Omega_0) \quad (1)$$

where $\upsilon_{\max}$ is the maximum edgewise growth rate of ferrite plates, ρ_c is the critical value of the radius of curvature at plate edges, D is the diffusion coefficient of carbon in austenite, and Ω_0 is solute supersaturation $(x_{\gamma\alpha} - x_0)/(x_{\gamma\alpha} - x_{\alpha\gamma})$. Here $x_{\gamma\alpha}$ is the equilibrium atomic fraction of carbon in austenite at the γ/α interface, $x_{\alpha\gamma}$ is the equilibrium atomic fraction of carbon in ferrite at the interface, and x_0 is the initial atomic fraction of carbon in austenite.

The Trivedi [16] equation is written as

$$\Omega_0 / \sqrt{(\pi p)}\mathrm{e}^{p} erfc(\sqrt{p}) = 1 + (\upsilon/\upsilon_c)\Omega_0 S_1(p) + (\rho_c/\rho)\Omega_0 S_2(p) \quad (2)$$

where $p = \upsilon p/D$ is the Peclet number, ρ is the actual curvature at the growth tip, S_1 and S_2 are the functions of p, and ρ_c/ρ decreases with Ω_0. The dependence of p on Ω_0 is given in Ref. [17].

According to Ref. [2], the growth rates of bainite in 0.48wt% carbon steel calculated by the Zener–Hillert and Bosze–Trivedi models are of order 10^{-3} mm/s during transformation at 330°C, which is consistent with the values measured in this study. Moreover, the average lengthening rate of all bainite plates measured in this study is 0.52×10^{-3} mm/s, which is on the same order as that given by Matas and Hehemann [5]. The growth rate of bainite plates is far smaller than the growth rate of martensite reported by Hsu (10^6 mm/s) [18] and is also smaller than the growth rate of pearlite given by Mehl and Hagel (10 mm/s) [19]. Therefore, the growth rate of bainite plates in the present study supports the diffusion transformation mechanism of bainite from the viewpoint of growth rate.

5. Conclusions

Dynamic *in situ* observation of the growth process in an Fe–C–Mn–Si superbainitic steel was conducted by high-temperature LSCM. The lengthening rates of bainite plates nucleating at different types of sites were measured during both cooling and isothermal transformations. The following conclusions can be drawn as follows.

(1) The lengthening rates of bainite plates during cooling and isothermal processes are different, and the growth rates of bainite plates that nucleated at different sites are also characterized by diversity.

(2) Bainite plates initiating at grain boundaries during cooling grow at higher rates, whereas those nucleating on preformed bainite grow at lower rates. However, the growth rate of plates nucleating at grain boundaries and within grains slows and speeds up during isothermal transformation.

(3) The growth rate of ferrite bainite measured in this study is consistent with the theoretical calculation results of the Zener–Hillert equation and the Trivedi equation. The growth rate of ferrite bainite is far lower than that of martensite and is also lower than that of pearlite. Therefore, the growth rate of ferrite bainite in the present study supports the diffusion transformation mechanism of bainite from the viewpoint of growth rate.

Acknowledgements

This work was financially supported by the National Natural Science Foundation of China (No. 51274154), the National High-Tech Research and Development Program of China (No. 2012AA03A504), the State Key Laboratory of Development and Application Technology of Automotive Steels (Baosteel Group), and the Key Project of Hubei Education Committee, China (No. 20121101).

References

[1] M. Chang and H. Yu, Kinetics of bainite-to-austenite transformation during continuous reheating in low carbon microalloyed steel, *Int. J. Miner. Metall. Mater.*, 20(2013), No. 5, p. 427.

[2] Y.Z. Zhu and J.P. Xu, A method to study interface diffusion of arsenic into a Nb–Ti microalloyed low carbon steel, *Int. J. Miner. Metall. Mater.*, 19(2012), No. 9, p. 821.

[3] H. Yada and T. Ooka, On the mechanism of bainite reaction: PT. 1. Investigation of the growth of bainite in Fe–Ni–C alloys by hot stage microscopy, *J. Jpn. Inst. Met.*, 31(1967), p. 766.

[4] H. Yada, M. Enomoto, and T. Sonoyama, Lengthening kinetics of bainitic plates in iron-nickel-carbon alloys, *ISIJ Int.*, 35(1995), No. 8, p. 976.

[5] S.J. Matas and R.F. Hehemann, The structure of bainite in hypoeutectoid steels, *Trans. Metall. Soc. AIME*, 221(1961), p. 179.

[6] M. Nemoto, *High Voltage Electron Microscopy*, Academic Press, New York, 1974, p. 230.

[7] D. Quidort and Y.J.M. Brechet, Isothermal growth kinetics of bainite in 0.5% C steels, *Acta Mater.*, 49(2001), No. 20, p. 4161.

[8] R.H. Goodenow, S.J. Matas, and R.F. Hehemann, Growth kinetics and mechanism of bainite transformation, *Trans. Metall. Soc. AIME*, 227(1963), p. 651.

[9] M.M. Rao and P.G. Winchell, Growth rate of bainite from low-carbon iron-nickel-carbon austenite, *Trans. Metall. Soc. AIME*, 239(1967), p. 956.

[10] J.M. Oblak and R.F. Hehemann, *Transformations and Hardenability in Steels*, Climax Molybdenum Company, Ann Arbor, MI, 1967, p. 15.

[11] G.R. Speich and M. Cohen, The growth rate of bainite, *Trans. Metall. Soc. AIME*, 218(1960), p. 1050.

[12] L. Kaufman, S.V. Radcliffe, and M. Cohen, *Decomposition of Austenite by Diffusional Processes*, John Wiley & Sons, New York, 1962, p. 313.

[13] M. Hillert, Diffusion and interface control of reactions in alloys, *Metall. Trans. A*, 6(1975), No. 1, p. 5.

[14] T. Ko and S.A. Cottrell, The formation of bainite, *J. Iron Steel Inst.*, 172(1952), p. 307.

[15] M. Hillert, The role of interfacial energy during solid state phase transformations, *Jernkontorets Annaler*, 141(1957), p. 757.

[16] R. Trivedi, The role of interfacial free energy and interface kinetics during the growth of precipitate plates and needles, *Metall. Trans.*, 1(1970), No. 4, p. 921.

[17] M. Enomoto, Thermodynamics and kinetics of the formation of widmanstätten ferrite plates in ferrous alloys, *Metall. Mater, Trans. A*, 25(1994), No. 9, p. 1947.

[18] T.Y. Hsu, *Martensite Transformation and Martensite*, Science Press, Beijing, 1980.

[19] R.F. Mehl and W.C. Hagel, The austenite: Pearlite reaction, *Prog. Met. Phys.*, 6(1956), p. 74.